



Pharmaceutical Nanotechnology

Influence of dextran on the bioadhesive properties of poly(anhydride) nanoparticles

Alina S. Porfire^a, Virginia Zabaleta^b, Carlos Gamazo^c, Sorin E. Leucuta^a, Juan M. Irache^{b,*}^a Department of Pharmaceutical Technology and Biopharmaceutics, University Iuliu-Hatieganu, 41V. Babes Str., 400023 Cluj-Napoca, Romania^b Department of Pharmacy and Pharmaceutical Technology, University of Navarra, 1 Irunlarrea Str., 31080 Pamplona, Spain^c Department of Microbiology, University of Navarra, 1 Irunlarrea Str., 31080 Pamplona, Spain

ARTICLE INFO

Article history:

Received 5 January 2009

Received in revised form 13 August 2009

Accepted 16 August 2009

Available online 25 August 2009

Keywords:

Dextran

Nanoparticles

Poly(anhydride)

Bioadhesion

Oral

ABSTRACT

This work describes the bioadhesive properties of poly(methyl vinyl ether-co-maleic anhydride) (Gantrez AN) nanoparticles (NP) associated with various types of dextran (two hydroxyl-functionalized dextrans and one amino-derivative of dextran). The association of dextran to the polymer was performed either prior NP formation or by the attachment of dextran to the surface of the just formed NP. The amount of dextran associated to the nanoparticles was quantified by a HPLC/ELSD method and dextran presence in the nanoparticles was confirmed by IR spectroscopy, ¹H NMR and *in vitro* agglutination assay. The *in vivo* bioadhesion study has demonstrated significantly higher adhesive interactions with the gastrointestinal tract of rats for all types of dextran associated nanoparticles compared with control nanoparticles. For nanoparticles associated with the aminated-dextran, the curves of bioadhesion were characterized by a maximum of adhesion just after administration followed by a rapid and constant decline with time. On the contrary, nanoparticles associated to conventional dextrans displayed a maximum bioadhesion between 1 and 3 h post-administration. These results encourage us for further use of these systems for oral delivery of drugs.

© 2009 Elsevier B.V. All rights reserved.

1. Introduction

In recent years, there has been a great interest in developing nanoparticulate systems in order to overcome some drawbacks of drug therapy, including poor bioavailability after oral administration of several drugs.

The orally administered particles may interact with the gastrointestinal surface and develop adhesive phenomena (mucoadhesion or bioadhesion), leading to an increase of their residence time in close contact with the mucosa or to a localization of the delivery system in a particular region of the gut (Irache et al., 2005). However, increasing the absorption efficiency of the orally administered nanoparticles is an important goal of many researchers. Thus, in the last years, several strategies have been developed including the association of nanoparticles with monoclonal antibodies specific for M cells (Pappo et al., 1991), their surface modification with lectins (Florence et al., 1995; Rodrigues et al., 2003) or polyethylene glycols (De Ascentiis et al., 1995; Yoncheva et al., 2007) and

their coating with mucoadhesive polymers (Takeuchi et al., 2001; Sarmento et al., 2007).

In this context, the development of polymeric carriers associated with polysaccharides has progressed recently. Among others, chitosans and dextrans appear to be the most popular polysaccharides for the modification of the surface of submicron carriers. In general, both compounds display a certain ability to develop adhesive interactions with different mucosal components (Bertholon et al., 2006a,b).

Chitosan is a deacetylated form of chitin comprising copolymers of glucosamine and N-acetyl glucosamine linked by β-(1–4) linkages (Borges et al., 2005). It appears that chitosan would promote the absorption of proteins across the mucosal surfaces due to its mucoadhesive properties and to its ability to induce a transient opening of the tight junctions (Illum et al., 1994; Van der Lubben et al., 2001). The adhesive properties of chitosan would be related with the development of electrostatic interactions with glycoproteins of mucus (Bertholon et al., 2006a). On the other hand, chitosan may also have an immunomodulatory effect as it has been shown to stimulate production of cytokines from immune cells (Otterlei et al., 1994) and enhance a naturally Th2/Th3-based microenvironment at the mucosal level in the absence of antigen (Porporatto et al., 2005).

Dextran is a polymer of glucose in which the glucosidic linkages are predominantly of the α-(1–6) type. Dextrans are amorphous

* Corresponding author at: Centro Galénico, Dep. Farmacia y Tecnología Farmacéutica, Universidad de Navarra, Irunlarrea, 1, 31080 Pamplona, Spain.
Tel.: +34 948 425600; fax: +34 948 425649.

E-mail address: jmirache@unav.es (J.M. Irache).

powders, freely soluble in water and are considered as inert in biological systems (Kojima et al., 1980; Williams and Taylor, 1992).

In fact, they are biodegraded by dextranases which are localized in various organs of human body (Wang et al., 2002; Prabu et al., 2008). Due to their beneficial properties, dextrans have largely been used in clinic for the prophylaxis of thrombosis and thromboembolism and for the prevention or treatment of hypovolemic shock (McBride et al., 1999; Williams and Taylor, 1992).

Concerning the use of dextrans in the field of nanoparticulate systems, the presence of dextran chains at the surface of nanoparticles or liposomes decreased the uptake of these systems by the mononuclear phagocyte systems and conferred them “stealth” properties (Passirani et al., 1998; Jaulin et al., 2000). Additionally, it has been reported that dextran coated nanoparticles possessed a certain ability to induce a steric repulsion for plasma proteins (Lemarchand et al., 2005).

Recently, our group of research have designed polymeric carriers based on a copolymer between methyl vinyl ether and maleic anhydride [poly(anhydride), Gantrez AN] and different types of dextran. Gantrez AN is a polymer widely used for pharmaceutical and medical purposes. In addition, it has been proposed as a suitable material for the preparation of nanoparticulate carriers with bioadhesive properties (Arbós et al., 2002b). Furthermore, various studies have shown that the modification of surface properties of this carrier lead to an increase of its affinity for the intestinal mucosa (Arbós et al., 2003).

The general aim of this work was to associate different types of dextran to poly(anhydride) nanoparticles, in order to obtain a particulate carrier with increased affinity for specific sites of the gastrointestinal tract. For this purpose, three different types of dextran were used: dextran with different molecular weights (40,000 and 70,000) and dextran with amino groups.

2. Materials and methods

2.1. Chemicals

Gantrez® AN 119 [poly(methyl vinyl ether-co-maleic anhydride); MW 200,000] was a gift from ISP (Barcelona, Spain). Dextran MW 70,000 (Dex70), dextran MW 40,000 (Dex40), rhodamine B isothiocyanate (RBITC), were purchased from Sigma–Aldrich Chemie (Germany). Aminodextran MW 70,000 (AmDex70) was obtained from Invitrogen (Spain). The simulated gastric (SGF; pH 1.2, pepsin 0.32%, w/v) and intestinal fluids (SIF; pH 7.5, pancreatin 1%, w/v) were prepared as described in USP XXVIII. All other chemicals used were of reagent grade and obtained from Merck (Spain).

2.2. Preparation of poly(anhydride) nanoparticles

Poly(methyl vinyl ether-co-maleic anhydride) or poly(anhydride) nanoparticles were prepared by a solvent displacement method (Arbós et al., 2002b). For dextran association, two different methods were assayed. Method A consisted of the incubation of the copolymer with either Dex40 or Dex70 in the organic phase of acetone, prior to nanoparticle formation by the addition of an ethanol–water mixture (1:1). The organic phase was then eliminated under reduced pressure (Buchi R-144, Switzerland).

Method B consisted of the preparation of unloaded poly(anhydride) nanoparticles, which were subsequently coated with dextran by incubation in water at room temperature.

In the case of Method A, the incubation times tested were 5, 15 and 30 min, while for the Method B, the previously formed nanoparticles were incubated with dextran aqueous solution for 30, 60 and 90 min.

In both cases, the nanoparticles were purified twice by centrifugation at 20,000 rpm, for 20 min (Sigma 3K30, Germany). The supernatants resulted in the purification steps were recovered in order to quantify the unloaded dextran by HPLC. For the bioadhesion study, the nanoparticles were fluorescently labeled by incubation with 1.25 mg of rhodamine B isothiocyanate (RBITC).

Finally, the nanoparticles were lyophilized using sucrose (5%) as cryoprotector. The control nanoparticles (NP) were prepared as described above without using dextran.

2.3. Characterization of the nanoparticles

2.3.1. Particle size, zeta potential and morphology

The particle size and zeta potential were determined by photon correlation spectroscopy and electrophoretic laser Doppler anemometry using a Zetamaster analyzer (Malvern Instruments, UK). For this purpose, samples were diluted with deionized water and measured at 25 °C with a scattering angle of 90°. The zeta potential was also measured in simulated gastric (pH 1.2) and intestinal (pH 7.5) fluids, prepared in the absence of enzymes.

The shape and morphology of the nanoparticles were assessed by scanning electron microscopy (SEM). Prior analysis, freeze-dried nanoparticles were resuspended in ultrapure water and centrifuged at 27,000 × g for 20 min at 4 °C. The supernatants (containing the cryoprotector) were rejected and the pellets were mounted on a glass plate adhered with an adhesive tape onto metal stubs and dried under hot flow air. Finally, the particles were covered with molecular gold in order to perform the SEM photographs.

2.3.2. Dextran analysis

The amount of dextran associated to the particles was determined by quantification of unloaded dextran in the supernatants obtained during the purification steps using a HPLC/ELSD method previously described (Zabaleta et al., 2007), with some minor modifications. Briefly, the separation of dextran was performed with an Agilent model 1100 series LC (Waldbronn, Germany) apparatus, using a PL Aquagel-OH column (300 nm × 7.5 mm), at 40 °C. The mobile phase consisted of a mixture of methanol and water in a gradient elution at a flow-rate of 1 ml/min. The detector used was an ELSD 2000 (Alltech, IL, USA), in the following conditions: drift tube temperature 110 °C and nitrogen flow 3 l/min. Aliquots of the supernatant obtained from the purification step by centrifugation were taken, diluted with double distilled water and 40 µl were injected into the chromatographic system.

Under these chromatographic conditions, no interferences between dextrans and the poly(anhydride) were observed. The retention times were 6.27 ± 0.03 min for Dex40 and 5.74 ± 0.05 min for Dex70. For both dextrans, calibration curves were performed in the range between 0.1 and 0.9 mg/ml. Detection and quantification limits were 0.025 and 0.1 mg/ml, respectively. The assay showed a polynomial relationship between the response and the corresponding concentration of dextran in the range of the calibration curve. The polynomial regression for Dex40 and Dex70 displayed correlation coefficients greater than 0.998 and 0.999 respectively. The accuracy values during the same day were lower than 15% for both dextrans at all of the concentrations tested.

The amount of dextran associated to the nanoparticles was calculated as the difference between the initial amount of dextran added and the amount of dextran determined in the supernatants.

In order to confirm dextran association to the poly(anhydride) nanoparticles, infrared spectroscopy (IR) and nuclear magnetic resonance (¹H NMR) analysis were performed. The infrared spectra were registered using Nicolet-FTIR Avatar 360 connected with OMNIC ESP software. On the other hand, ¹H NMR spectra were obtained in a Bruker Avance 400 spectrometer (Germany). For this purpose, exact amounts of samples were dissolved in deuter-

ated DMSO (dimethyl sulfoxide) and the spectra were obtained at $n_s = 6400$. The analyzed samples were dextran associated nanoparticles and free dextran, all of them being processed in the same ratio and experimental conditions.

2.3.3. Aminodextran analysis

To confirm the association of AmDex70 to the nanoparticles, *in vitro* agglutination assay of NP-AmDex70 with concanavalin A was used. This study was performed by measuring the turbidity change, as a function of time, at 405 nm (Labsystems iEMS Reader MF, Finland), after co-incubation of 1 mg/ml nanoparticles aqueous suspension with 1 mg/ml of concanavalin A solution in water.

2.3.4. RBITC quantification

The amount of RBITC loaded into the nanoparticles was determined by colorimetry at wavelength 540 nm (Labsystems iEMS Reader MF, Finland). The RBITC loading was calculated using the concentration found after total hydrolysis of 2 mg nanoparticles in 0.1N NaOH for 24 h at 37 °C.

The release of RBITC from nanoparticles was determined after incubation of 10 mg particles in 1 ml of simulated gastric medium (pH 1.2) at 37 °C for 2 h followed up by 24 h of incubation in 1 ml of simulated intestinal medium (pH 7.4). These media were prepared as described in USP XXVIII.

For quantification, standard curves of RBITC in 0.1N NaOH were used (concentration range of 0.5–30 mg/ml; $r > 0.999$).

2.4. Bioadhesion studies

The bioadhesion study was performed using a protocol previously described (Arbós et al., 2002a), in compliance with the regulations of the responsible Committee of the University of Navarra in line with the European legislation on animal experiments (86/609/EU). RBITC loaded nanoparticles were administered orally to male Wistar rats fasted overnight (average weight 225 g, Harlan, Spain), divided in groups of 3 animals each. The animals were housed under normal conditions and 12 h before the experiment were placed in metabolic cages and fasted overnight but with free access to water.

Each animal received a single oral dose of 1 ml aqueous suspension containing 10 mg nanoparticles loaded with RBITC (approximately 45 mg particles/kg body weight). The animals were sacrificed by cervical dislocation at 0.5, 1, 3 and 8 h post-administration. The abdominal cavity was opened and the stomach, small intestine and cecum were removed. Then, the gut was divided into six anatomical regions: stomach (Sto), intestine (I1, I2, I3 and I4) and cecum (Ce). Each segment was opened lengthwise along the mesentery and rinsed with phosphate buffered saline (pH 7.4). Further, the stomach, small intestine and cecum were cut into segments of 2 cm length and digested in 1 ml 3N NaOH for 24 h. RBITC was extracted from the digested samples by addition of 2 ml methanol, vortexed for 1 min and centrifuged at 4000 rpm for 10 min. Aliquots (1 ml) of the resulted supernatants were assayed for RBITC by spectrofluorimetry at λ_{ex} 540 nm and λ_{em} 580 nm (GENios, TECAN, Austria) in order to calculate the fraction of adhered nanoparticles to the mucosa. For calculations, standard curves of RBITC were prepared by addition of RBITC-solutions in 3N NaOH (0.5–10 μ g/ml) to tissue segments following the same treatment steps ($r > 0.996$).

For each nanoparticle formulation, the total adhered fraction of the nanoparticles in the whole gastrointestinal tract was plotted vs. time. From these curves, the following parameters of bioadhesion were estimated: the maximal amount of nanoparticles adhered to the gut surface (Q_{max}), the area under the curve of bioadhesion from 0 to 8 h post-administration (AUC_{adh}), the mean residence time of the adhered fraction of nanoparticles in the mucosa (MRT_{adh}) and

the terminal elimination rate of the adhered fraction (K_{adh}). All of these parameters were calculated with the WinNonlin 1.5 software (Pharsight Corporation, USA).

2.5. Statistical analysis

The bioadhesion data and physico-chemical characteristics were compared using Student's *t*-test. *p* values of <0.05 were considered significant. All calculations were performed using SPSS® statistical software program (SPSS® 10, Microsoft, USA).

3. Results and discussion

3.1. Optimization of preparation method and characterization of dextran–poly(anhydride) nanoparticles

Dextran–poly(anhydride) nanoparticles were prepared by two different methods in order to study the different possibilities to obtain the higher degree of association between dextran and the polymer nanoparticles. In this optimization process, three main parameters were evaluated: type of dextran (dextran 40, dextran 70 and aminated-dextran 70), method of preparation (Method A and Method B, see Section 2) and the incubation time between the polysaccharide and the polymer or the just formed nanoparticles. In a preliminary work, the bulk concentration of dextran (expressed as the ratio between the polysaccharide and the copolymer) was fixed at a ratio of 0.20 by weight. When dextran/poly(anhydride) ratios higher than 0.20 (by weight) were used in the preparation process, the average dextran association efficiency decreased.

Fig. 1 shows the influence of the preparation method and of the incubation time on the dextran association to nanoparticles. When

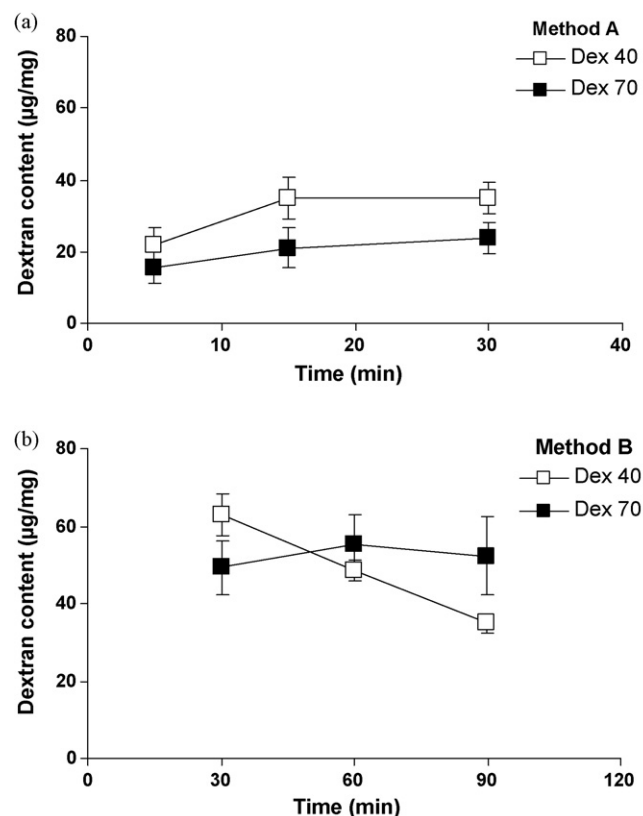


Fig. 1. Influence of the preparation method and of the incubation time on either dextran 40 (Dex40) or dextran 70 (Dex70) association to poly(anhydride) nanoparticles. Nanoparticles were obtained by Method A (a) and Method B (b). Experimental conditions: dextran/poly(anhydride) ratio of 0.20 by weight.

nanoparticles were prepared by “Method A” (incubation between the polysaccharide and the copolymer between the formation of nanoparticles), the amount of associated dextran to the resulting nanoparticles slightly increased by increasing the incubation time. In any case, the amount of polysaccharide associated to nanoparticles was higher for Dex40 than for Dex70. On the other hand, when nanoparticles were prepared by “Method B” (incubation of nanoparticles with dextrans), depending on the polysaccharide used, a different behavior was observed. Thus, for Dex40, the degree of dextran association decreased by increasing the time of incubation. On the contrary, for Dex70, little modifications of dextran content were observed by prolonging the time of incubation from 30 to 90 min. In any case, Method B provided a higher degree of association between dextran and poly(anhydride) nanoparticles than “Method A” (about 2–3 times higher).

The optimum incubation time was found to be 30 min for both methods and both types of dextran.

For AmDex70, the presence of amino functional groups resulted in a high reactivity with the acid anhydride residues of Gantrez AN. This fact is in agreement with previous results described by Yoncheva et al. (2007) that obtained higher pegylation degrees of poly(anhydride) nanoparticles when using amino-functionalized poly(ethylene glycols) (PEGs) than with conventional (hydroxy-functionalized) PEGs. As a result, dextran-nanoparticles prepared with this amino-derivative were only prepared by Method B and, in this case, the selected dextran/poly(anhydride) ratio was 0.003. In order to confirm the presence of functional aminodextran on the surface of the nanoparticles, the concanavalin A agglutination test was performed. This test showed a turbidity increase that was found to be double for NP-AmDex70 than for control nanoparticles, confirming the presence of amino groups on the surface of the nanoparticles.

On the basis of these results, some formulations were selected for further characterization and bioadhesion study. The formulations selected were: NP-AmDex70 (prepared by Method B with 0.3 mg AmDex70 and incubation time 1 h); NP-Dex70b (prepared by Method B with 20 mg Dex70, 30 min of incubation); NP-Dex70a (prepared by Method A with 20 mg Dex70, 30 min of incubation); NP-Dex40b (prepared by Method B with 20 mg Dex40, 30 min of incubation).

Table 1 summarizes the main physico-chemical properties of these formulations. All the formulations displayed a homogeneous size of about 150 nm and low polydispersity. These measurements were confirmed by SEM analysis, in which the nanoparticles displayed a spherical shape (Fig. 2). The zeta potential values were negative and similar for all the formulations tested. This fact was also observed when zeta potential was measured in simulated gastric and intestinal conditions (SGF and SIF without enzymes). Under acidic conditions the zeta potential for all the dextran-nanoparticles was very low (ranged from –5 to –8 mV), whereas under simulated intestinal conditions, these parameters were around –35 mV (data not shown). These results appeared to confirm the chemical interaction between the primary amine residues of AmDex70 and the anhydride group of the copolymer.

Concerning the amount of dextran associated to nanoparticles, NP-Dex70b displayed a dextran content that was found to be approximately 2 times higher ($p < 0.05$) than for NP-Dex70a nanoparticles (49 vs. 24 $\mu\text{g}/\text{mg}$ NP). Also, the association of Dextran 40 was significantly higher than that of Dextran 70 using the same preparation conditions ($p < 0.05$ for NP-Dex70b vs. NP-Dex40b). On the contrary, there were no differences concerning the RBITC loading between the selected formulations.

Fig. 3 shows the overlaid IR spectra of dextran, conventional nanoparticles and dextran associated nanoparticles. The intense bands observed at 1780 and 1850 cm^{-1} are characteristics for the

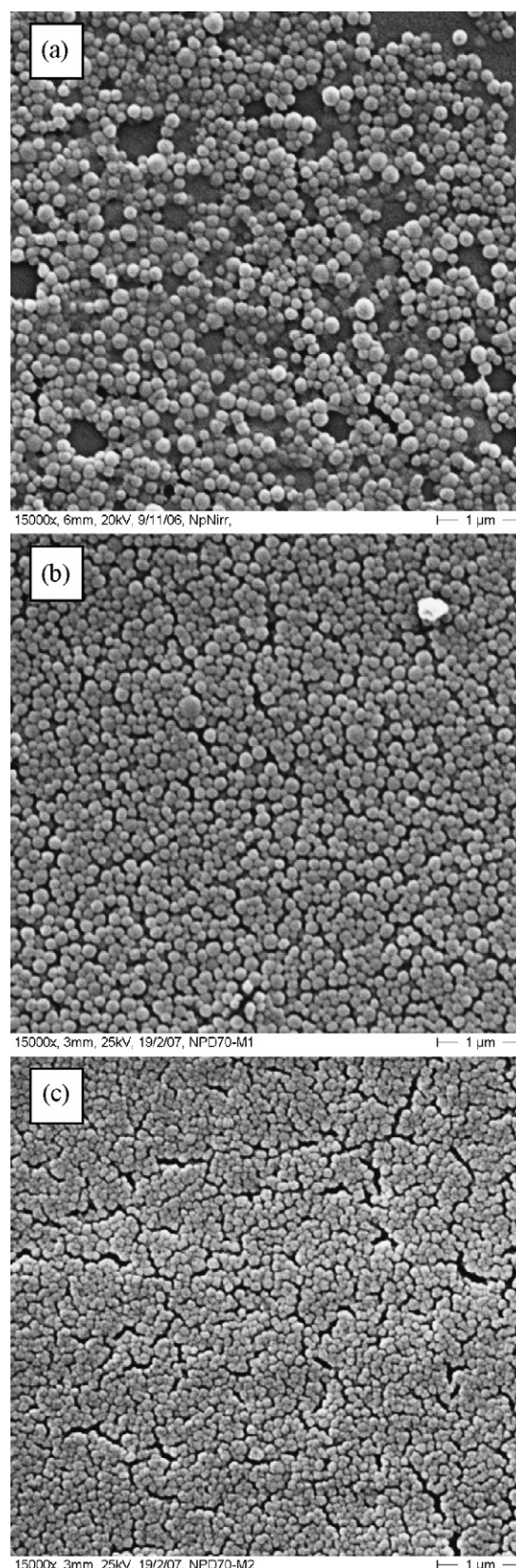


Fig. 2. Scanning electron microscopy (SEM) for lyophilized (a) NP, (b) NP-Dex70a and (c) NP-Dex70b.

Table 1Physico-chemical properties of dextran associated nanoparticles. Data are expressed as mean \pm S.D., $n = 6$.

Sample	Size (nm)	Zeta potential (mV)	Dextran content ($\mu\text{g}/\text{mg NP}$) ^a	RBITC content ($\mu\text{g}/\text{mg NP}$) ^b
NP	140 \pm 1.5	−26 \pm 1.0	–	17.2 \pm 0.5
NP-AmDex70	155 \pm 0.6	−26 \pm 2.5	n.d.	16.6 \pm 0.7
NP-Dex70b	155 \pm 2.1	−28 \pm 1.2	49.2 \pm 6	15.1 \pm 0.5
NP-Dex70a	124 \pm 0.6	−30 \pm 1.8	23.8 \pm 4	17.5 \pm 0.6
NP-Dex40b	150 \pm 1.5	−31 \pm 3.5	62.8 \pm 6	14.4 \pm 0.2

^a Quantity of dextran loaded to the nanoparticles ($\mu\text{g}/\text{mg}$) determined by HPLC/ELSD method.^b RBITC content in $\mu\text{g}/\text{mg}$ nanoparticles, measured by colorimetry.

anhydride group of Gantrez AN. The spectrum clearly demonstrates the association of dextran to the nanoparticles, as indicated by the following typical bands for dextran present in the spectrum of the nanoparticles: a broad absorption band at 3400 cm^{-1} , distinctive for OH groups of dextran, the glycosidic C–H band at 2900 cm^{-1} and the peculiar absorption band for the C–O–C linkage in the dextran ring around 1630 cm^{-1} . However, no apparent chemical covalent bonds between the two compounds (dextran and polymer) were detected in the spectra of nanoparticles. By ^1H NMR we could also evidence dextran association to the particles.

On the other hand, by ^1H NMR analysis (Fig. 4), two types of peaks characteristics for dextrans (dextran 40 and dextran 70) were visualized. The first peak corresponded to the protons of methylene units of dextran (at 4.85 ppm), whereas another 3 peaks (between 4.5 and 4.95 ppm) were characteristics of the hydroxylic protons of dextran. Again, the spectra of dextran-nanoparticles did not clearly reveal any type of covalent bond between the –OH groups of dextran and the anhydride groups of the polymer. All of these observations appear to suggest that the association between either dextran 40 or dextran 70 with the poly(anhydride) is mediated by physical entrapment in the core of the nanoparticles and/or adsorption at their surface. Comparing with polyethyleneglycols (PEG), dextrans would show a lower reactivity with the anhydride groups of the copolymer. In fact, using PEG 2000 and methoxy-PEG 2000, Yoncheva et al. (2005, 2007) demonstrated by ^1H NMR that pegylation of poly(anhydride) nanoparticles occurs by means of a direct reaction between the terminal hydroxyl of PEG and the anhydride groups of Gantrez AN.

3.2. Bioadhesion studies

In vivo bioadhesion studies were performed using RBITC loaded nanoparticles (10 mg, approximately 45 mg particles/kg

body weight), that were administered perorally to male Wistar rats fasted overnight.

To ensure that the fluorescence determined in the gastrointestinal parts was due to the fluorescence of the nanoparticles, *in vitro* release of RBITC was evaluated. The percentage of RBITC released in 2 h in simulated gastric fluid was around 10% and 20% in simulated intestinal fluid. Therefore, it was assumed that the fluorescence detected in the gastrointestinal tract was due to the RBITC-associated to the nanoparticles.

Fig. 5 represents the gut distribution of the adhered fractions of dextran associated to poly(anhydride) nanoparticles (NP-AmDex70, NP-Dex70a, NP-Dex70b and NP-Dex40b) and control nanoparticles (NP), as a function of time. All the formulations tested displayed a higher degree of association with the gut mucosa during the first 1 h than after a long time post-administration. In addition, it was observed a homogeneous distribution in the whole gut for all the formulations tested, without any marked specificity for a particular region of the gut. In any case, all the nanoparticle formulations, irrespective of the presence and type of dextran, displayed a tendency to concentrate in the stomach mucosa and, in a high degree, in the upper regions of the small intestine (duodenum and jejunum). Overall, NP-AmDex70 showed the highest ability to develop bioadhesive interactions (Fig. 5b); although, the amount of nanoparticles decreased rapidly with time. On the contrary, for NP-Dex70b and NP-Dex40b, a significant amount of the given dose of nanoparticles remained adhered to the jejunum and ileum of animals (I2–I4 portions in Fig. 5d and e) 3 h post-administration.

Fig. 6 shows the curves of bioadhesion obtained by representing the total amount of the adhered particles to the whole gastrointestinal tract over time, whereas Table 2 summarizes the parameters of bioadhesion for the different formulations tested, calculated from the curves of bioadhesion. Concerning the curves, it was clear that the formulations could be ascribed to one of the two different

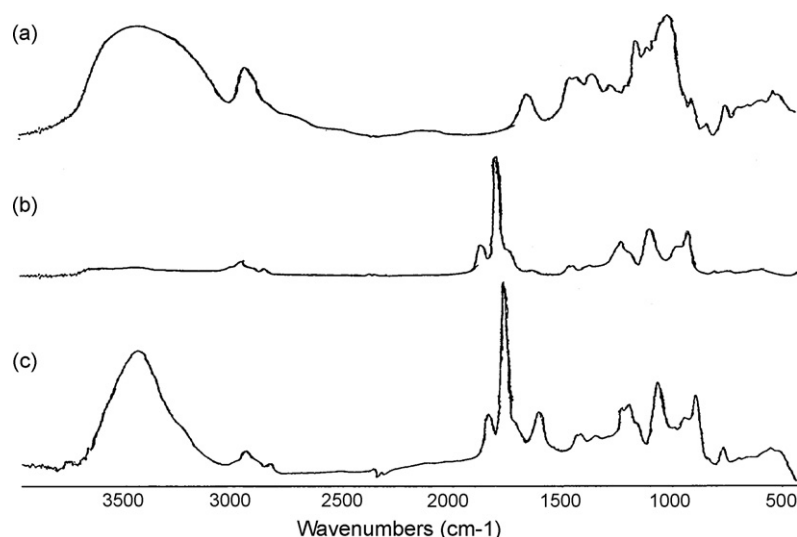


Fig. 3. Infrared spectra of (a) dextran; (b) conventional poly(anhydride) nanoparticles and (c) dextran associated poly(anhydride) nanoparticles (NP-Dex70a).

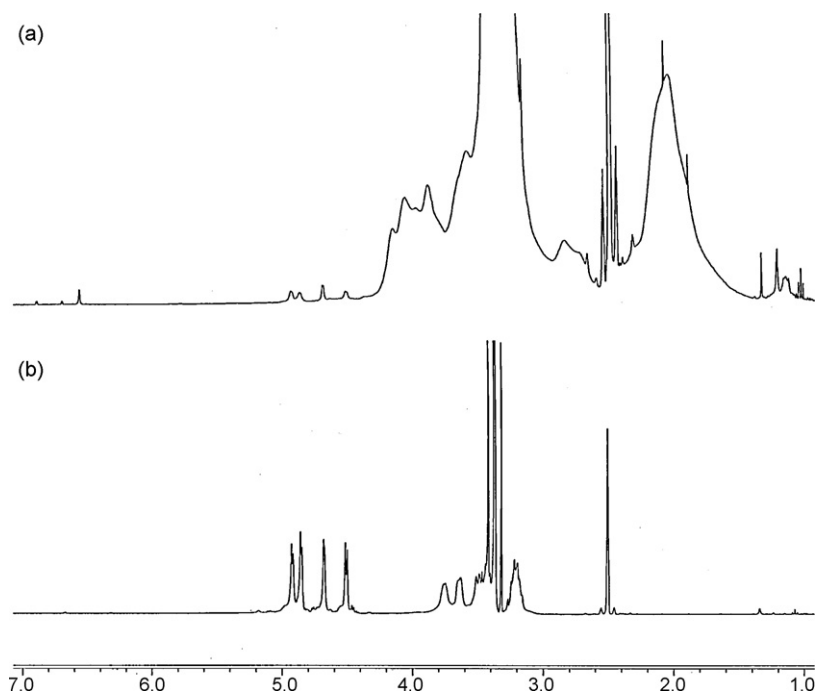


Fig. 4. ^1H NMR spectra of NP-Dex40b (top) and free dextran (bottom) obtained in DMSO at $n_s = 6400$.

profiles of bioadhesion observed. Thus, for NP, NP-AmDex70 and NP-Dex70a, the profile was characterized by an initial maximum of bioadhesion followed by a rapid decline of the amount of the adhered particles to the whole gut mucosa. Interestingly, this maximum of bioadhesion was higher for NP-AmDex70 than for the other formulations. In this case, more than 55% of the given dose of NP-AmDex70 was recovered adhered to the mucosa, whereas for NP or NP-Dex70a this value was only about 35% (Table 2).

On the other hand, for NP-Dex40b and NP-Dex70b, a different profile of the curve of bioadhesion was found. In this case, the curves were characterized by an increase of the adhered amount of nanoparticles which reach the maximum in the period ranged from 1 and 3 h post-administration.

Concerning the intensity of the adhesive interactions (AUC_{adh}), all the dextran associated nanoparticles displayed significantly higher values of AUC_{adh} than control nanoparticles ($p < 0.05$), suggesting an improvement in the intensity of the adhesion due to dextran association. On the other hand, the higher elimination rate of the adhered fraction was found for NP-Dex70b and NP-AmDex70. Finally, all the formulations had similar residence times of the adhered fraction to the mucosa (MRT), around 3–3.7 h.

From these results some conclusions can be drawn. All types of nanoparticles tested in our experiment were able to develop

bioadhesive interactions with the gastrointestinal tract of animals, mainly following two types of bioadhesion profiles. Moreover, we could observe that all dextran associated nanoparticles showed a higher bioadhesive capacity than control nanoparticles. It is clear that the type of dextran and the method used for nanoparticle preparation are the main factors that influenced their behavior in the gastrointestinal tract of rats. Thus, nanoparticles prepared with Method B showed a prolonged interaction with the gut mucosa while nanoparticles prepared with Method A had a profile similar to that of control nanoparticles, characterized by a decrease of the initial adhesion capacity in time. This observation sustained our assumption that preparing the nanoparticles with Method B would lead to dextran association at their surface, which will become more hydrophilic, while by Method A the nanoparticles would have the dextran mostly distributed in the core of nanoparticles.

In general, it seemed that dextran association to the nanoparticles facilitates the diffusion through the mucus layer due to the higher hydrophilicity conferred leading to stronger adhesive interactions with the gut mucosa. These results agree well with previous observations that the association of poly(anhydride) with hydrophilic molecules such as polyethylene glycols (Yoncheva et al., 2007) and thiamine (Salman et al., 2007) leads to

Table 2
Bioadhesion parameters, derived from the curves of bioadhesion.

Treatment	Q_{max}^a (mg)	$\text{AUC}_{\text{adh}}^b$ (mg h)	K_{adh}^c (h^{-1})	MRT^d (h)
NP	3.25 ± 0.43	12.23 ± 0.97	0.15 ± 0.05	3.17 ± 0.32
NP-AmDex70	$5.45 \pm 0.61^{**}$	$17.74 \pm 1.48^{**}$	0.25 ± 0.06	3.40 ± 0.64
NP-Dex70b	3.95 ± 0.84	$19.41 \pm 1.26^{**}$	0.21 ± 0.13	3.00 ± 0.30
NP-Dex70a	3.37 ± 0.39	$15.56 \pm 1.31^*$	0.16 ± 0.05	3.54 ± 0.59
NP-Dex40b	3.12 ± 0.38	$16.22 \pm 1.72^*$	0.13 ± 0.08	3.66 ± 0.60

^a Maximal amount of particles adhered to the gut mucosa.

^b Area under the curve of bioadhesion.

^c Terminal elimination rate of the adhered fraction.

^d Mean residence time of the adhered fraction of nanoparticles in contact with the mucosa.

* $p < 0.05$ for dextran associated nanoparticles vs. control nanoparticles (NP).

** $p < 0.01$ for dextran associated nanoparticles vs. control nanoparticles (NP).

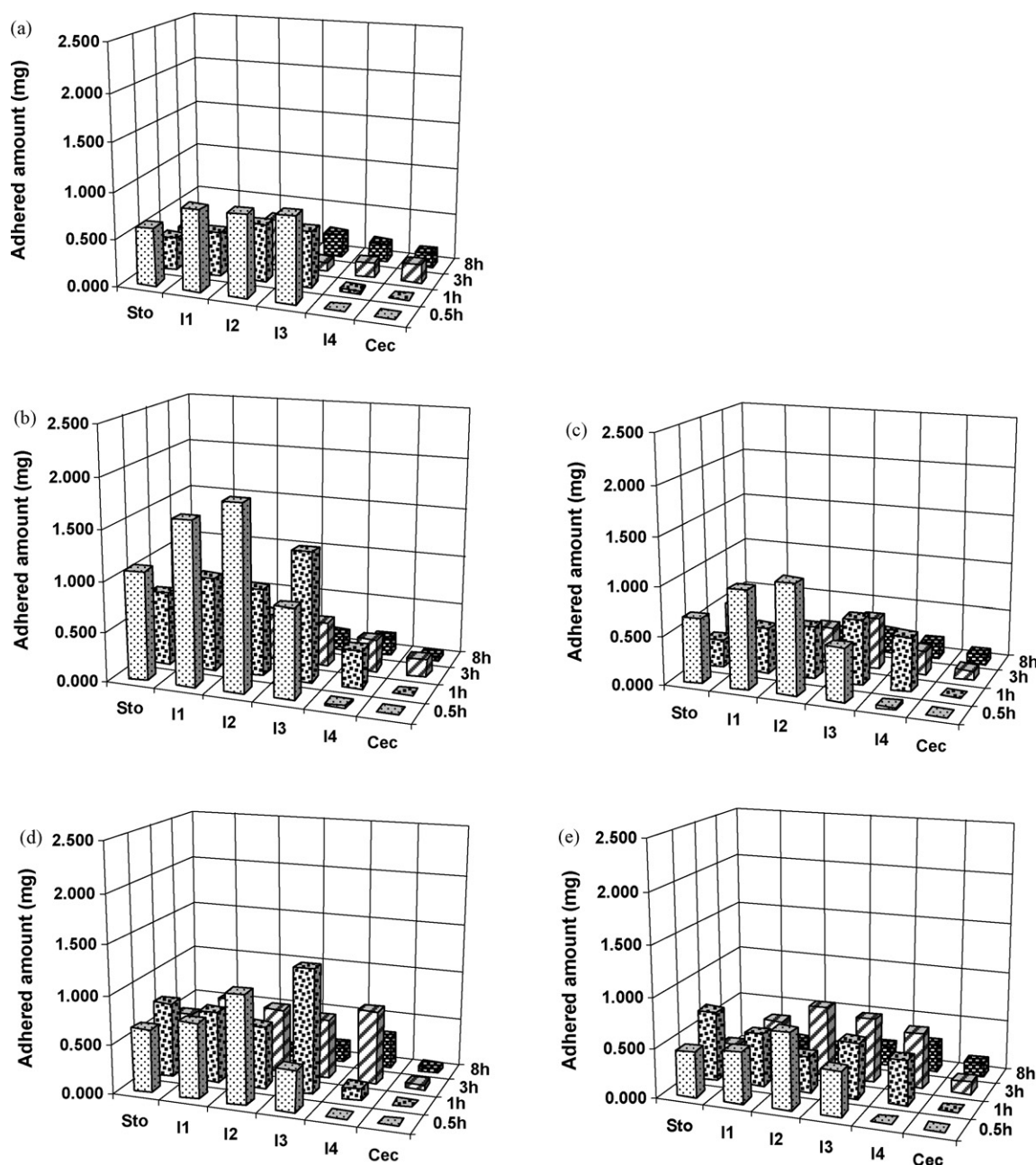


Fig. 5. Evolution of the amount of adhered nanoparticles within the gut of rats after the oral administration of a single dose of 10 mg RBITC loaded nanoparticles. (a) Control nanoparticles (NP); (b) NP-AmDex70; (c) NP-Dex70a; (d) NP-Dex70b; (e) NP-Dex40b. Each value represents the mean of 3 experiments.

a higher intensity of the bioadhesive interactions developed. In addition, all of these bioadhesive carriers were characterized by a discrete initial capacity to develop bioadhesive interactions and a maximum of adhesion between 1 and 3 h post-administration.

On the contrary, when AmDex70 was associated to Gantrez nanoparticles the profile of adhesion was similar to that obtained by Arbós et al. (2002a) for BSA-coated poly(anhydride) nanoparticles, with an initial maximum of adhesion (30 min post-administration), followed by a decrease of the adhered fraction along the time. Also, the intensity of the bioadhesive phenomena calculated as AUC_{adh} was approximately 1.5 times higher for both AmDex70 and BSA-nanoparticles than for plain poly(anhydride) nanoparticles. Therefore, it is plausible to speculate that the interactions between NP-AmDex70 and the gut mucosa would be mainly restricted to the upper area of the mucosa. Similarly, this different

behavior of NP-AmDex70 (compared with conventional dextran-nanoparticles) would be ascribed to a different conformation of the aminodextran on the surface of nanoparticles after its chemical interaction with the anhydride group of the copolymer. This fact would agree with previous data concerning the mucoadhesiveness of chitosans (Fernandez-Urrusuno et al., 1999; Sogias et al., 2008), which are also characterized by the presence of primary amino groups.

On the other hand, dextran-poly(anhydride) nanoparticles (NP-Dex70 and NP-Dex40), as for pegylated nanoparticles, would be capable to minimise their interaction with components of the intestinal lumen or with the mucus layer. This fact would facilitate their "filtration" through the intestinal content and their interaction directly with the surface of the enterocytes. Obviously, this would be the reason for which the maximum of bioadhesion appears later than for NP-AmDex70 or control nanoparticles.

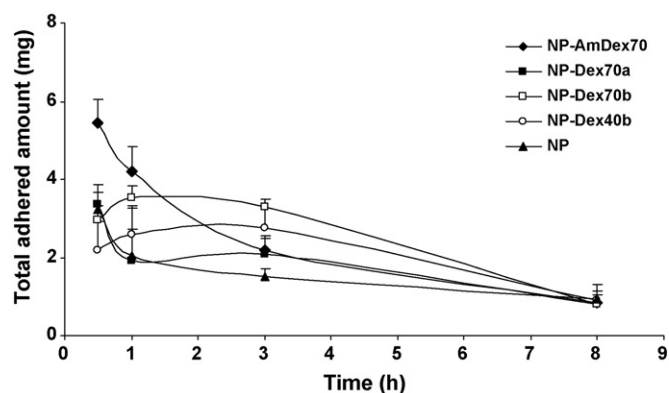


Fig. 6. Curves of bioadhesion representing the total adhered amount of nanoparticles in the whole gastrointestinal tract over time, after the oral administration of 10 mg nanoparticles. Data are expressed as mean \pm S.D. ($n=3$ for each time of the experiment).

4. Conclusion

This work has demonstrated the possibility to associate different types of dextran to poly(anhydride) nanoparticles by two simple methods. The higher association degree of dextran was achieved when nanoparticles were coated with the low molecular weight dextran or the dextran functionalized with amino groups. Even if no chemical linkage between conventional dextrans and the copolymer could be identified by spectral analysis, it seems that the interactions between both compounds are strong enough to influence the bioadhesion properties of the non-associated nanoparticles. All types of dextran-nanoparticles had significantly higher affinity for the gastrointestinal tract of rats than control nanoparticles. However, their behavior was influenced by the presence of functional groups. Thus, for NP-AmDex70, the maximum of bioadhesion was found 30 min post-administration when close to 60% of the given dose was found adhered to the gut mucosa. On the other hand, for NP-Dex70 or NP-Dex40, the maximum of bioadhesion took place between 1 and 3 h post-administration.

Acknowledgements

This work was supported by grants from the “Instituto de Salud Carlos III” (number: PI070326; Res. 15/10/2007) and Department of Health of the “Gobierno de Navarra” (Res. 2118/2007) in Spain. Alina Porfire was also financially supported by grants from The National University Research Council (number TD278/2007, ID457/2007) and Ministry of Education, Research and Youth in Romania.

References

Arbós, P., Arango, M.A., Campanero, M.A., Irache, J.M., 2002a. Quantification of the bioadhesive properties of protein-coated PVM/MA nanoparticles. *Int. J. Pharm.* 242, 129–136.

Arbós, P., Campanero, M.A., Arango, M.A., Renedo, M.J., Irache, J.M., 2003. Influence of the surface characteristics of PVM/MA nanoparticles on their bioadhesive properties. *J. Controlled Release* 89, 19–30.

Arbós, P., Wirth, M., Arango, M.A., Gabor, F., Irache, J.M., 2002b. Gantrez AN as a new polymer for the preparation of ligand–nanoparticle conjugates. *J. Controlled Release* 83, 321–330.

Bertholon, I., Ponchel, G., Labarre, D., Couvreur, P., Vauthier, C., 2006a. Bioadhesive properties of poly(alkylcyanoacrylate) nanoparticles coated with polysaccharide. *J. Nanosci. Nanotechnol.* 6, 3102–3109.

Bertholon, I., Vauthier, C., Labarre, D., 2006b. Complement activation by core-shell poly(isobutylcyanoacrylate)-polysaccharide nanoparticles: influences of surface morphology, length, and type of polysaccharide. *Pharm. Res.* 23, 1313–1323.

Borges, O., Borchard, G., Verhoef, J.C., De Sousa, A., Junginger, H.E., 2005. Preparation of coated nanoparticles for a new mucosal vaccine delivery system. *Int. J. Pharm.* 299, 155–166.

De Ascentiis, A., De Grazia, J.L., Bowman, C.N., Colombo, P., Peppas, N.A., 1995. Mucoadhesion of poly(2-hydroxyethyl methacrylate) is improved when linear poly(ethylene oxide) chains are added to the polymer network. *J. Controlled Release* 33, 197–201.

Fernandez-Urrusuno, R., Romani, D., Calvo, P., Vila-Jato, J.L., Alonso, M.J., 1999. Development of a freeze-dried formulation of insulin-loaded chitosan nanoparticles intended for nasal administration. *S.T.P. Pharm. Sci.* 9, 429–436.

Florence, A.T., Hillery, A.M., Hussain, N., Jani, P.U., 1995. Nanoparticles as carriers for oral peptide absorption: studies on particle uptake and fate. *J. Controlled Release* 36, 39–46.

Illum, L., Farraj, N.F., Davis, S.S., 1994. Chitosan as a novel nasal delivery system for peptide drugs. *Pharm. Res.* 11, 1186–1189.

Irache, J.M., Huici, M., Konecny, M., Espuelas, S., Campanero, M.A., Arbós, P., 2005. Bioadhesive properties of Gantrez nanoparticles. *Molecules* 10, 126–145.

Jaulin, N., Appel, M., Passirani, C., Barratt, G., Labarre, D., 2000. Reduction of the uptake by a macrophagic cell line of nanoparticles bearing heparin or dextran covalently bound to poly(methyl methacrylate). *J. Drug Target.* 8, 165–172.

Kojima, T., Hashida, M., Muranishi, S., Sezaki, H.J., 1980. Mitomycin C-dextran conjugate: a novel high molecular weight pro-drug of mitomycin C. *J. Pharm. Pharmacol.* 32, 30–34.

McBride, L.R., Naunheim, K.S., Fiore, A.C., Moroney, D.A., Swartz, M.T., 1999. Clinical experience with 111 thoratec ventricular assist devices. *Ann. Thorac. Surg.* 67, 1233–1238.

Lemarchand, C., Gref, R., Lesieur, S., Hommel, H., Vacher, B., Besheer, A., Maeder, K., Couvreur, P., 2005. Physico-chemical characterization of polysaccharide-coated nanoparticles. *J. Controlled Release* 108, 97–111.

Otterlei, M., Varum, K.M., Ryan, L., Espevik, T., 1994. Characterization of binding and TNF-alpha-inducing ability of chitosans on monocytes: the involvement of CD14. *Vaccine* 12, 825–832.

Pappo, J., Ermark, T.H., Steger, H.J., 1991. Monoclonal antibody-directed targeting of fluorescent polystyrene microsphere to Peyer's patch M cells. *Immunology* 73, 277–280.

Passirani, C., Barratt, G., Devissaguet, J.P., Labarre, D., 1998. Long-circulating nanoparticles bearing heparin or dextran covalently bound to poly(methyl methacrylate). *Pharm. Res.* 15, 1046–1050.

Porporatto, C., Bianco, I.D., Correa, S.G., 2005. Local and systemic activity of the polysaccharide chitosan at lymphoid tissues after oral administration. *J. Leukoc. Biol.* 78, 62–69.

Prabu, P., Chaudhari, A.A., Aryal, S., Dharmaraj, N., Park, S.Y., 2008. In vitro evaluation of poly(caprolactone) grafted dextran (PGD) nanoparticles with cancer cell. *J. Mater. Sci.: Mater. Med.* 19, 2157–2163.

Rodrigues, J.S., Santos-Magalhaes, N.S., Coelho, L.C.B.B., Couvreur, P., Ponchel, G., Gref, R., 2003. Novel core (polyester)-shell (polysaccharide) nanoparticles: protein loading and surface modification with lectins. *J. Controlled Release* 92, 103–112.

Salman, H.H., Gamazo, C., Agüeros, M., Irache, J.M., 2007. Bioadhesive capacity and immunoadjuvant properties of thiamine-coated nanoparticles. *Vaccine* 25, 8123–8132.

Sarmiento, B., Ribeiro, A., Veiga, F., Ferreira, D., Neufeld, R., 2007. Oral bioavailability of insulin contained in polysaccharide nanoparticles. *Biomacromolecules* 10, 3054–3060.

Sogias, I.A., Williams, A.C., Khutoryansky, V.V., 2008. Why is chitosan mucoadhesive? *Biomacromolecules* 9, 1837–1842.

Takeuchi, H., Yamamoto, H., Kawashima, Y., 2001. Mucoadhesive nanoparticulate systems for peptide drug delivery. *Adv. Drug Deliv. Rev.* 47, 39–54.

Van der Lubben, I.M., Verhoef, J.C., Van Aelst, A., Borchard, G., Junginger, H.E., 2001. Chitosan microparticles for oral vaccination: preparation, characterization and preliminary in vivo uptake studies in murine Peyer's patches. *Biomaterials* 22, 687–694.

Wang, L.Q., Tu, K., Li, Y., Zhang, J., Jiang, L., Zhang, Z., 2002. Synthesis and characterization of temperature responsive graft copolymers of dextran with poly(N-isopropylacrylamide). *React. Funct. Polym.* 53, 19–27.

Williams, A.S., Taylor, G., 1992. Synthesis, characterization and release of cromoglycate from dextran conjugates. *Int. J. Pharm.* 83, 233–239.

Yoncheva, K., Lizarraga, E., Irache, J.M., 2005. Pegylated nanoparticles based on poly(methyl vinyl ether-co-maleic anhydride): preparation and evaluation of their bioadhesive properties. *Eur. J. Pharm. Sci.* 24, 411–419.

Yoncheva, K., Guembe, L., Campanero, M.A., Irache, J.M., 2007. Evaluation of bioadhesive potential and intestinal transport of pegylated poly(anhydride) nanoparticles. *Int. J. Pharm.* 334, 156–165.

Zabaleta, V., Campanero, M.A., Irache, J.M., 2007. An HPLC with evaporative light scattering detection method for the quantification of PEGs and Gantrez in PEGylated nanoparticles. *J. Pharm. Biomed. Anal.* 44, 1072–1078.